Asociación Argentina
de Mecánica Computacional

Mecánica Computacional Vol XXVII, págs. 2497-2513 (artículo completo)
Alberto Cardona, Mario Storti, Carlos Zuppa. (Eds.)
San Luis, Argentina, 10-13 Noviembre 2008

TOPOLOGY OPTIMIZATION OF THREE-DIMENSIONAL ELASTIC STRUCTURES USING BOUNDARY ELEMENTS

Adrián P. Cisilino[a], Christine Bertsch[b] and Néstor Calvo[c]

[a] *División Soldadura y Fractomecánica INTEMA, CONICET,*
Facultad de Ingeniería - Universidad Nacional de Mar del Plata, Av. Juan B. Justo 4302,
(7600) Mar del Plata, cisilino@fi.mdp.edu.ar

[b] *Institut für Angewandte Mechanik, Technische Universität Braunschweig*
P.O. Box 3329 Pockelstr. 14 D-38106 Braunschweig, Germany

[c] *Centro Internacional de Métodos Computacionales en Ingeniería – CONICET,*
Güemes 3450, 3000 Santa Fe, Argentina

Keywords: Topology optimization, Topological derivative, Boundary elements, Elasticity.

Abstract. Topological optimization provides a powerful framework to obtain the optimal domain topology for several engineering problems. The topological derivative is a function which characterizes the sensitivity of a given problem to the change of its topology, like opening a small hole in a continuum or changing the connectivity of rods in a truss.
A numerical approach for the topological optimization of three-dimensional linear elastic problems using boundary elements is presented in this work. The topological derivative is computed from strain and stress results which are solved by means of a standard boundary element analysis. Models are discretized using linear or constant elements and a periodic distribution of internal points over the domain. The total potential energy is selected as cost function. The evaluation of the topological derivative is performed as a post-processing procedure. Afterwards, material is removed from the model by deleting the internal points and boundary nodes with the lowest values of the topological derivate. The new geometry is then remeshed creating “holes” at those positions where internal points and boundary points have been removed. The procedure is repeated until a given stopping criterion is satisfied.
The proposed strategy proved to be flexible and robust. A number of examples are solved and results are compared to those available in the literature.

1 INTRODUCTION

Structural optimization is a major concern in the design of mechanical systems. The classical design problem consists in finding the optimum geometric configuration of a body that maximizes or minimizes a given cost function while it satisfies the problem boundary conditions. The typical approaches for solving this problem are size and shape techniques (Cea et al., 2000). In size optimization only the cross sections of the structure are optimized, making this approach specially suited for the optimization of beam/bar structures. On the other hand, in shape optimization techniques the optimal geometry is searched within a class of domains having the same topology as the initial design, that is, no holes are introduced in the optimization domain.

Topology optimization is a relatively new and growing field of structural optimization which has widespread in both academic and real-life industrial problems (Bendsøe y Sigmund, 2004). The goal in topology optimization is to find the material distribution that minimizes some objective function subject to given constraints on the amount of material available. The shape and the connectivity of the domain are both design variables; so that the introduction of new boundaries is permitted (and expected). This versatile approach is capable of delivering optimal designs with a priori poor information on the optimal shape of the structure, and it possess the ability of producing the best overall structure (Tanskanen, 2002). Thus, topology optimization features a larger space of feasible solutions and can play an important role in the conceptual design phase of the engineering life cycle (Vegamenti et al., 2005).

Homogenization methods are possibly the most used approach for topology optimization (Bendsøe and Kikuchi, 1988). In these methods a material model with micro-scale voids is introduced and the topology optimization problem is defined by seeking the optimal porosity of such a porous medium using one of the optimality criteria. In this way, the homogenization technique is capable of producing internal holes without prior knowledge of their existence. However, the homogenization method often produces designs with infinitesimal pores that make the structure not manufacturable. A number of variations of the homogenization method have been investigated to deal with these issues, such as penalization of intermediate densities and filtering procedures (Sigmund and Peterson, 1998). On the other hand, there exist the so-called level set methods which are based on the moving of free boundaries (Wang and Wang, 2004;Wang and Wang, 2006). Although very effective, the main drawback of level set methods is that they require of pre-existent holes within the model domain in order to conduct a topology optimization.

The topological derivative provides an alternative approach for shape optimization. It was firstly introduced by Ceá et al. (1974) by combining a fixed point method with the natural extension of the classical shape gradient. The basic idea behind the topological derivative is the evaluation of cost function sensitivity to the creation of a hole. In this way, wherever this sensitivity is low enough (or high enough depending on the nature of the problem) the material can be progressively eliminated. Topological derivative methods aim to solve the aforementioned limitations of the homogenization methods.

A numerical approach for the topological optimization of three-dimensional elastic problems using boundary elements is presented in this work. The formulation of the problem is based on recent results by Novotny et al. (2007), who introduced a new procedure for computing the topological derivative for three-dimensional problems which allows overcoming some mathematical difficulties involved in its classical definition. The boundary element analysis is done using a standard direct formulation. Models are discretized using constant quadrilateral elements and a periodic distribution of internal points over the domain.

The total strain energy is selected as cost function. The problem is solved incrementally. In every step, material is removed from the model by deleting the internal points with the lowest values of the topological derivate. The new geometry is automatically remeshed using an algorithm capable of detecting "holes" at those positions where internal points have been removed. In this way, the procedure avoids using intermediate densities, the classical limitation of the homogenization methods. The procedure is repeated until a given stopping criterion is satisfied. The performance of the proposed strategy is illustrated for a number of examples and their results compared to solutions available in the literature.

Although the finite element method has been the main numerical tool for the implementation of topology optimization techniques, there are implementations using the Boundary Element Method (BEM) (Marckerle, 2003) and free boundary parameterization methods (Wang and Wang, 2006). The antecedent in the implementation of the Novotny et al. (2003) approach for the computation of the topological derivative using BEM is two-dimensional. These are the works by Marczak (2007) and Cisilino (2006) for potential problems and by Marczak (2006) and Carretero and Cisilino (2008) for elastic problems. Both implementations, those due to Marczak (2006, 2007) and those due to Cisilino (2006) and Carretero and Cisilino (2008) use similar procedures for the computation of the topological derivative results. However, they differ in the strategy proposed for the creation of the holes and the model update and remeshing. The procedures introduced in the work by Carretero and Cisilino (2008) for two-dimensional elasticity are extended here to three-dimensional problems.

2 GENERAL SPECIFICATIONS

The classical definition of the topological derivative relates the sensitivity of a cost function $\psi(\Omega)$ when the topology of the optimization domain Ω is altered by creating a small cavity or hole. Consider with this purpose a bounded three-dimensional domain Ω with smooth boundary $\partial\Omega$. The domain is perturbed by introducing a small spherical hole of radius ε at an arbitrary position *x*. Therefore, we have the original domain without hole and the new perturbed domain $\Omega_\varepsilon = \Omega - B_\varepsilon$ with boundary $\partial\Omega_\varepsilon = \partial\Omega \cup \partial B_\varepsilon$, where B_ε and ∂B_ε denote the domain and the boundary of the hole respectively (see Figure 1). The topological derivative, D_T, associated to a given cost function ψ defined in both domains is given by

$$D_T(\mathbf{x}) = \lim_{\varepsilon \to 0} \frac{\psi(\Omega_\varepsilon) - \psi(\Omega)}{f(\varepsilon)}, \tag{1}$$

where $f(\varepsilon)$ is a negative function that decreases monotonically so that $f(\varepsilon) \to 0$ with $\varepsilon \to 0^+$.

However, the direct application and implementation of equation (1) comprises some mathematical difficulties because it is not possible to establish a homeomorphism (or mapping) between the domains with different topologies (domains with and without the hole).

Novotny et al. (2007) proposed an alternative definition of the D_T that overcomes the problem. They developed the so-called topological-shape sensitivity method which based on the mathematical framework developed for shape sensitivity analysis. Novotny et al. (2007) demonstrate that if $f(\varepsilon)$ is chosen in order to ensure $0 < |D_T(\mathbf{x})| < \infty$ the topological derivative given in (1) can be written as

$$D_T(\mathbf{x}) = \lim_{\varepsilon \to 0} \frac{1}{f'(\varepsilon)} \frac{d}{d\tau} \psi(\Omega_\tau) \Big|_{\tau=0}, \tag{2}$$

where τ is real positive number used to parameterize the domain Ω_τ such that

$$\mathbf{x}_\tau = \mathbf{x} + \tau \mathbf{v}, \quad \mathbf{x}_\tau\big|_{\tau=0} = \mathbf{x}, \quad \Omega_\tau\big|_{\tau=0} = \Omega_\varepsilon. \tag{3}$$

The symbol $\mathbf{v}$ in equation (3) defines the shape change velocity which is a smooth vector field in Ω_ε with the following values on the boundary $\partial\Omega_\varepsilon$

$$\begin{cases} \mathbf{v} = -\mathbf{n} & \text{on } \partial B_\varepsilon \\ \mathbf{v} = 0 & \text{on } \partial\Omega \end{cases} \tag{4}$$

where $\mathbf{n}$ stands for the outward normal unit vector (see Figure 1).

Finally, the shape sensitivity of the cost function in relation to the domain perturbation characterized by velocity field $\mathbf{v}$ is given by

$$\frac{d}{d\tau} \psi(\Omega_\tau) \Big|_{\tau=0} = \lim_{\tau \to 0} \frac{\psi(\Omega_\tau) - \psi(\Omega_\varepsilon)}{\tau}. \tag{5}$$

The topological-shape sensitivity method presented above provides an effective means for computing the topological derivative. Since it is possible to associate the domain perturbation with the parameter τ, such that $\delta\varepsilon = \|x_\tau - x\|$ so that $\delta\varepsilon = \tau$, the domain Ω_ε with $\tau = 0$ can be seen as the material configuration while the domain Ω_τ can be regarded as the spatial configurations. In fact, the domains Ω_ε and Ω_τ have the same topology, and so it is now possible to establish a homeomorphic map between them.

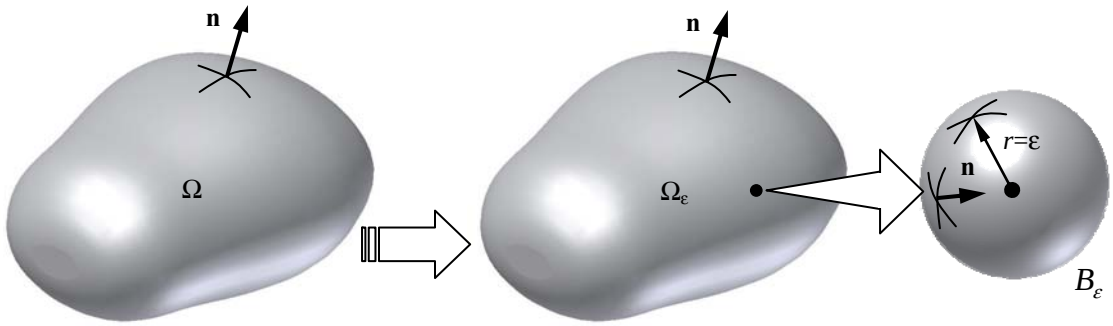

Figure 1: The topological-shape sensitivity analysis: (a) Original domain Ω, (b) Perturbed domain Ω_ε and (c) Small hole in the perturbed domain B_ε.

3 THE TOPOLOGICAL DERIVATIVE FOR THREE-DIMENSIONAL ELASTICITY

In the present work the D_T is applied to the optimization of three dimensional elastostatics considering a mechanical model restricted to infinitesimal strains and displacements with a linear isotropic constitutive relation. The basic outline for the derivation of the topological derivative expression for three-dimensional elasticity by means of the topological-shape sensitivity method is presented next following Novotny et al. (2007).

The derivation of the topological derivative equations require to state the equilibrium equations in the original domain without the hole, Ω, and the perturbed domain with the

hole, Ω_ε. The mechanical model for the original domain without the hole can be stated via its variational formulation as following: given the domain Ω with boundary $\partial\Omega = \Gamma_N \cup \Gamma_D$ submitted to a set of surface tractions $\bar{\mathbf{t}}$ on the Neumann boundary Γ_N and displacements constraints $\bar{\mathbf{u}}$ on the Dirichlet boundary Γ_D, find the displacement vector field $\mathbf{u}$ such that

$$\int_\Omega \boldsymbol{\sigma}(\mathbf{u}) \cdot \boldsymbol{\varepsilon}(\mathbf{w})\, d\Omega = \int_{\Gamma_N} \bar{\mathbf{t}} \cdot \mathbf{w}\, d\Gamma\,, \tag{6}$$

where $\mathbf{w}$ stands for the field of admissible displacement variations which satisfies the condition $\mathbf{w} = 0$ on Γ_D, $\boldsymbol{\varepsilon} = \frac{1}{2}\left(\nabla\mathbf{u} + \nabla\mathbf{u}^T\right)$ is the Green deformation tensor and $\boldsymbol{\sigma} = \mathbf{C}\boldsymbol{\varepsilon}$ is the Cauchy stress tensor where $\mathbf{C}$ is the elasticity tensor (see for example Gurtin, 1981).

The Euler-Lagrange equation associated to the variational problem in equation (6) is given by the following boundary value problem:

$$\begin{cases} \text{find } \mathbf{u} \text{ such that} \\ \\ \operatorname{div} \boldsymbol{\sigma}(\mathbf{u}) = 0 \text{ in } \Omega \\ \\ \mathbf{u} = \bar{\mathbf{u}} \text{ on } \Gamma_D \\ \\ \boldsymbol{\sigma}(\mathbf{u}) \cdot \mathbf{n} = \bar{\mathbf{t}} \text{ on } \Gamma_N \end{cases} \tag{7}$$

Similarly, the mechanical model for the domain Ω_ε with a hole B_ε can be stated via its variational formulation as following: find the displacement vector field $\mathbf{u}_\varepsilon$ such that

$$\int_{\Omega_\varepsilon} \boldsymbol{\sigma}_\varepsilon(\mathbf{u}_\varepsilon) \cdot \boldsymbol{\varepsilon}_\varepsilon(\mathbf{w}_\varepsilon)\, d\Omega_\varepsilon = \int_{\Gamma_N} \bar{\mathbf{t}} \cdot \mathbf{w}_\varepsilon\, d\Gamma\,. \tag{8}$$

In accordance with the variational problem given in equation (8) null tractions, $\boldsymbol{\sigma}_\varepsilon(\mathbf{u}_\varepsilon) \cdot \mathbf{n} = 0$, are specified on the hole boundary, ∂B_ε (homogeneous Neumann boundary condition).

The cost function ψ is, in a certain way, arbitrary. The total strain energy is adopted as cost function in this work and the differentiation method will be adopted to compute its shape derivative. Considering the total potential energy written in the spatial configuration Ω_τ, then $\psi(\Omega_\tau) = \Im(\mathbf{u}_\tau)$ with

$$\Im(\mathbf{u}_\tau) = \frac{1}{2}\int_{\Omega_\tau} \boldsymbol{\sigma}_\tau(\mathbf{u}_\tau) \cdot \boldsymbol{\varepsilon}_\tau(\mathbf{u}_\tau)\, d\Omega_\tau - \int_{\Gamma_N} \bar{\mathbf{t}} \cdot \mathbf{u}_\tau\, d\Gamma_\tau\,, \tag{9}$$

where the domain integral in the right represents the total strain energy stored in the body and the boundary integral represents the external work. This objective function is equivalent to optimize the mean compliance of the problem.

In addition, $\mathbf{u}_\tau$ is the solution of the variational problem defined in the configuration Ω_τ, that is: find the displacement vector field $\mathbf{u}_\tau$ such that

$$\int_{\Omega_\tau} \boldsymbol{\sigma}_\tau(\mathbf{u}_\tau) \cdot \boldsymbol{\varepsilon}_\tau(\mathbf{w}_\tau)\, d\Omega_\tau = \int_{\Gamma_N} \bar{\mathbf{t}} \cdot \mathbf{w}_\tau\, d\Gamma\,. \tag{10}$$

The Reynolds' transport theorem (Gurtin, 1981) and the concept of material derivatives

of spatial fields is used to compute the shape derivative of the cost function $\psi(\Omega_\tau)$ at $\tau=0$. That is

$$\left.\frac{d}{d\tau}\Im(\mathbf{u}_\tau)\right|_{\tau=0} = \frac{1}{2}\int_{\partial\Omega_\varepsilon}\left[\boldsymbol{\sigma}_\varepsilon(\mathbf{u}_\varepsilon)\cdot\boldsymbol{\varepsilon}_\varepsilon(\mathbf{u}_\varepsilon)\right](\mathbf{v}\cdot\mathbf{n})\,d\Gamma$$
$$+\frac{1}{2}\int_{\Omega_\varepsilon}\frac{\partial}{\partial\tau}\left[\boldsymbol{\sigma}_\tau(\mathbf{u}_\tau)\cdot\boldsymbol{\varepsilon}_\tau(\mathbf{u}_\tau)\right]\Big|_{\tau=0} d\Omega_\varepsilon - \int_{\Gamma_N}\bar{\mathbf{t}}\cdot\frac{d\mathbf{u}_\varepsilon}{d\tau}d\Gamma \tag{11}$$

It is worth noting that the stress-strain constitutive relationship $\boldsymbol{\sigma}=\mathbf{C}\boldsymbol{\varepsilon}$ is constant in relation to τ.

Taking into account that

$$\frac{\partial(\cdot)}{\partial\tau} = \left.\frac{d(\cdot)}{d\tau}\right|_{\mathbf{x}_\tau \text{ fixed}}, \tag{12}$$

and considering that $\mathbf{u}_\varepsilon$ is the solution of equation (8) (and consequently of the associated Euler-Lagrange equation) and that its derivative $d\mathbf{u}_\varepsilon/d\tau$ can be written as

$$\frac{d\mathbf{u}_\varepsilon}{d\tau} = \frac{\partial\mathbf{u}_\varepsilon}{\partial\tau} + (\nabla\mathbf{u}_\varepsilon)\cdot\mathbf{v}, \tag{13}$$

the expression in equation (11) can be written as (for further details please see Novotny et al. (2007)):

$$\left.\frac{d}{d\tau}\Im(\mathbf{u}_\tau)\right|_{\tau=0} = \int_{\partial\Omega_\varepsilon}\left\{\frac{1}{2}\left[\boldsymbol{\sigma}_\varepsilon(\mathbf{u}_\varepsilon)\cdot\boldsymbol{\varepsilon}_\varepsilon(\mathbf{u}_\varepsilon)\right]\mathbf{I} - (\nabla\mathbf{u}_\varepsilon)^T\boldsymbol{\sigma}_\varepsilon(\mathbf{u}_\varepsilon)\right\}(\mathbf{n}\cdot\mathbf{v})\,d\Gamma, \tag{14}$$

which becames an integral defined on the boundary $\partial\Omega_\varepsilon$. The symbol $\mathbf{I}$ in equation (14) is the second order identity tensor. Besides, it is worth noting that the expression into {} corresponds to that of the Eshelby energy-momentum tensor (see for instance Gurtin (1981)).

From the definition of the velocity field in equation (4) and taking into account the homogeneous Neumann boundary condition on ∂B_ε, equation (14) can be written as

$$\left.\frac{d}{d\tau}\Im(\mathbf{u}_\tau)\right|_{\tau=0} = -\int_{\partial\Omega_\varepsilon}\left[\frac{1}{2}\boldsymbol{\sigma}_\varepsilon(\mathbf{u}_\varepsilon)\cdot\boldsymbol{\varepsilon}_\varepsilon(\mathbf{u}_\varepsilon) - \boldsymbol{\sigma}_\varepsilon(\mathbf{u}_\varepsilon)\mathbf{n}\cdot(\nabla\mathbf{u}_\varepsilon)\mathbf{n}\right]d\Gamma$$
$$= -\frac{1}{2}\int_{\partial\Omega_\varepsilon}\boldsymbol{\sigma}_\varepsilon(\mathbf{u}_\varepsilon)\cdot\boldsymbol{\varepsilon}_\varepsilon(\mathbf{u}_\varepsilon)\,d\Gamma. \tag{15}$$

The expression for the topological derivative results after replacing equation (15) into equation (2):

$$D_T(\mathbf{x}) = -\frac{1}{2}\lim_{\varepsilon\to 0}\frac{1}{f'(\varepsilon)}\int_{\partial\Omega_\varepsilon}\boldsymbol{\sigma}_\varepsilon(\mathbf{u}_\varepsilon)\cdot\boldsymbol{\varepsilon}_\varepsilon(\mathbf{u}_\varepsilon)\,d\Gamma. \tag{16}$$

The calculation of the limit in equation (16) requires of an asymptotic analysis in order to know the behavior of the stress and strain fields when $\varepsilon\to 0$. This behavior is obtained from the analytical solution for a stress distribution around a spherical void (Sadowsky, 1949). Besides, and in accordance with resulting the asymptotic behavior of expression (16), the function $f(\varepsilon)$ must be chosen such that

$$f(\varepsilon) = -|\partial\Omega_\varepsilon| = -4\pi\varepsilon^2 . \tag{17}$$

in order to take the limit $\varepsilon \to 0$.

Then, the final expression for the topological derivative becomes a scalar function which depends on the solution of displacement field solution, $\mathbf{u}$, associated to the original domain Ω. This expression can be written in terms of the stress tensor $\boldsymbol{\sigma}$:

$$D_T(\mathbf{x}) = \frac{3(1-\nu)}{4(7-5\nu)E}\left\{10(1+\nu)\boldsymbol{\sigma}(\mathbf{u})\cdot\boldsymbol{\sigma}(\mathbf{u}) - (1+5\nu)\left[\operatorname{tr}\boldsymbol{\sigma}(\mathbf{u})\right]^2\right\}, \tag{18}$$

or in terms of the stress $\boldsymbol{\sigma}$ and strain $\boldsymbol{\varepsilon}$ tensors:

$$D_T(\mathbf{x}) = \frac{3(1-\nu)}{4(7-5\nu)E}\left[10\boldsymbol{\sigma}(\mathbf{u})\cdot\boldsymbol{\varepsilon}(\mathbf{u}) - \frac{1-5\nu}{1-2\nu}\operatorname{tr}\boldsymbol{\sigma}(\mathbf{u})\ \operatorname{tr}\varepsilon(\mathbf{u})\right], \tag{19}$$

where E and ν are the Young modulus and the Poisson ratio respectively. It is worth noting that equations 18 and 19 are only valid for the linear elastic case.

4 BOUNDARY ELEMENT IMPLEMENTATION

The implemented algorithm solves the optimization problem incrementally by progressively removing a small portion of the domain per step (usually known as *hard kill* algorithm (Eschenauer and Olhoff, 2001). The algorithm was implemented as a framework in C++, which includes the class *BEMSolver* for the boundary element analysis.

It is worth noting that since the D_T is a function of the stress and strains only, its evaluation does not require any special BEM implementation. With this purpose a three-dimensional BEM solver with constant quadrilateral elements was implemented. The solver is based on the standard BEM formulation for elasticity (see for instance Aliabadi and Wrobel, 2002). The models are discretized using a regular mesh like that illustrated in Figure 2*a*. The boundary mesh is accompanied by a regular array of internal points where the local D_T values are computed in a post-processing procedure. Every internal point represents a cubic cell of material which can be removed during the optimization (see Figure 2*b*).

The incremental algorithm consisting in the progressive removal of material from the model will lead to extinction of the optimization domain if no stopping criterion is specified. Two stopping criteria used in this work: a goal minimum material volume fraction, $\gamma_{\min} = \operatorname{vol}\left(\Omega^{\text{final}}\right) \Big/ \operatorname{vol}\left(\Omega^{0}\right)$, or a maximum limit displacement for given point.

The algorithm can be summarized as follows (the index j stands for the step number):

i. Provide an initial domain $\Omega^{j=0}$ and the stopping criterion.
ii. Solve the BEM model for the Ω^j domain. Compute the stress $\boldsymbol{\sigma}$ and strain $\boldsymbol{\varepsilon}$ fields at internal and boundary points.
iii. Compute the $D_T(x)$ using the formulas (18) or (19).
iv. Select the points with the minimum values of D_T (a few percent of the total number of points).
v. Create holes by removing the points selected in step iv.
vi. Remesh BEM model and validate its geometrical integrity. If necessary, fix the model geometry.

vii. Check stopping criterion. If necessary, make $j = j+1$, define a new domain Ω^j, and go to step ii.
viii. At this stage the desired final topology is obtained.

Model discretization and remeshing

The strategies for the model discretization and remeshing are key issues for the performance of the implemented algorithm. The BEM mesh is constructed in every optimization step from the spatial distribution of internal points. As it has been mentioned earlier, every internal point represents a cubic material cell. The optimization algorithm eliminates a number of internal points in every step, what results in the deactivation of the cells they are associated to. In this way the material is progressively removed from the model. The boundary for the new model geometry is constructed in every step by identifying the faces of the active cells (that is, those cells associated to the internal points which are still present in the model discretization) which belong to one cell only (faces shared by two cells do not belong to the model boundary). Finally, each of the boundary faces is assimilated to a quadrilateral constant boundary element with the geometry given by four geometrical nodes and the functional node in the centroid (see detail in Figure 2*a*).

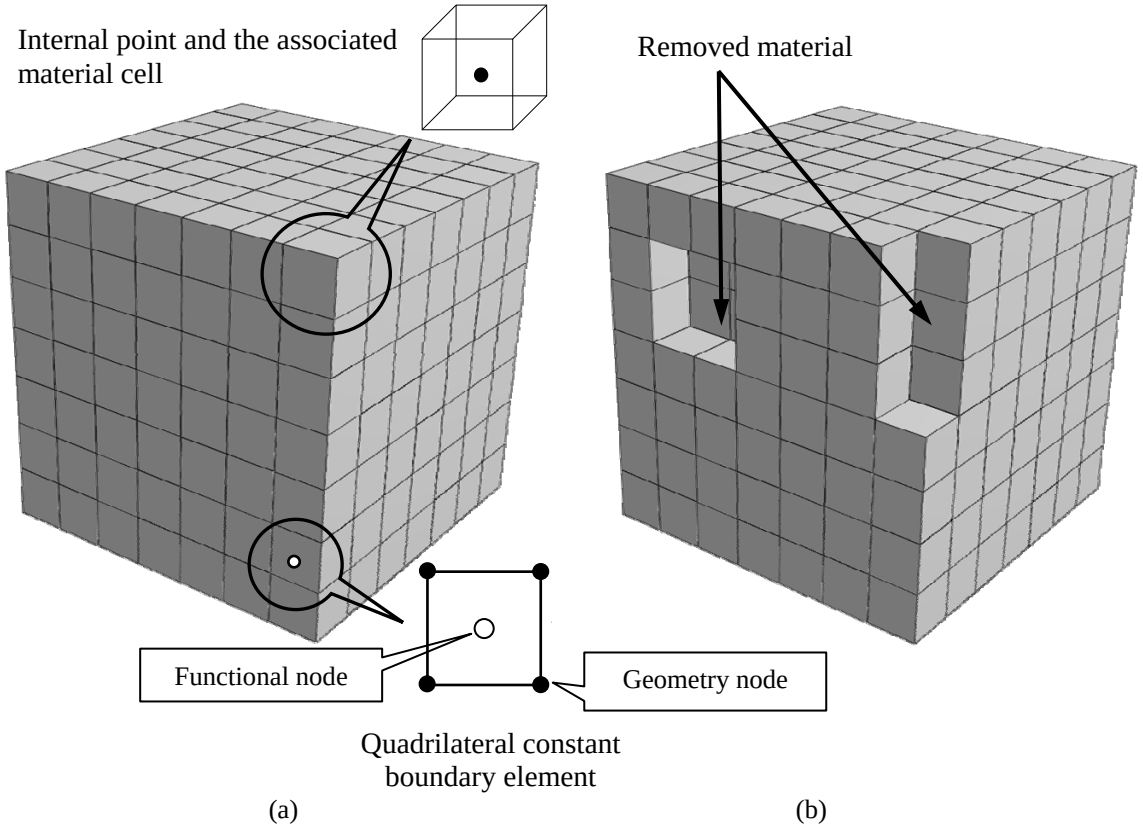

Figure 2: BEM discretization strategy: (a) Initial discretization using constant quadrilateral elements and internal points, (b) Modified domain after the removal of internal points.

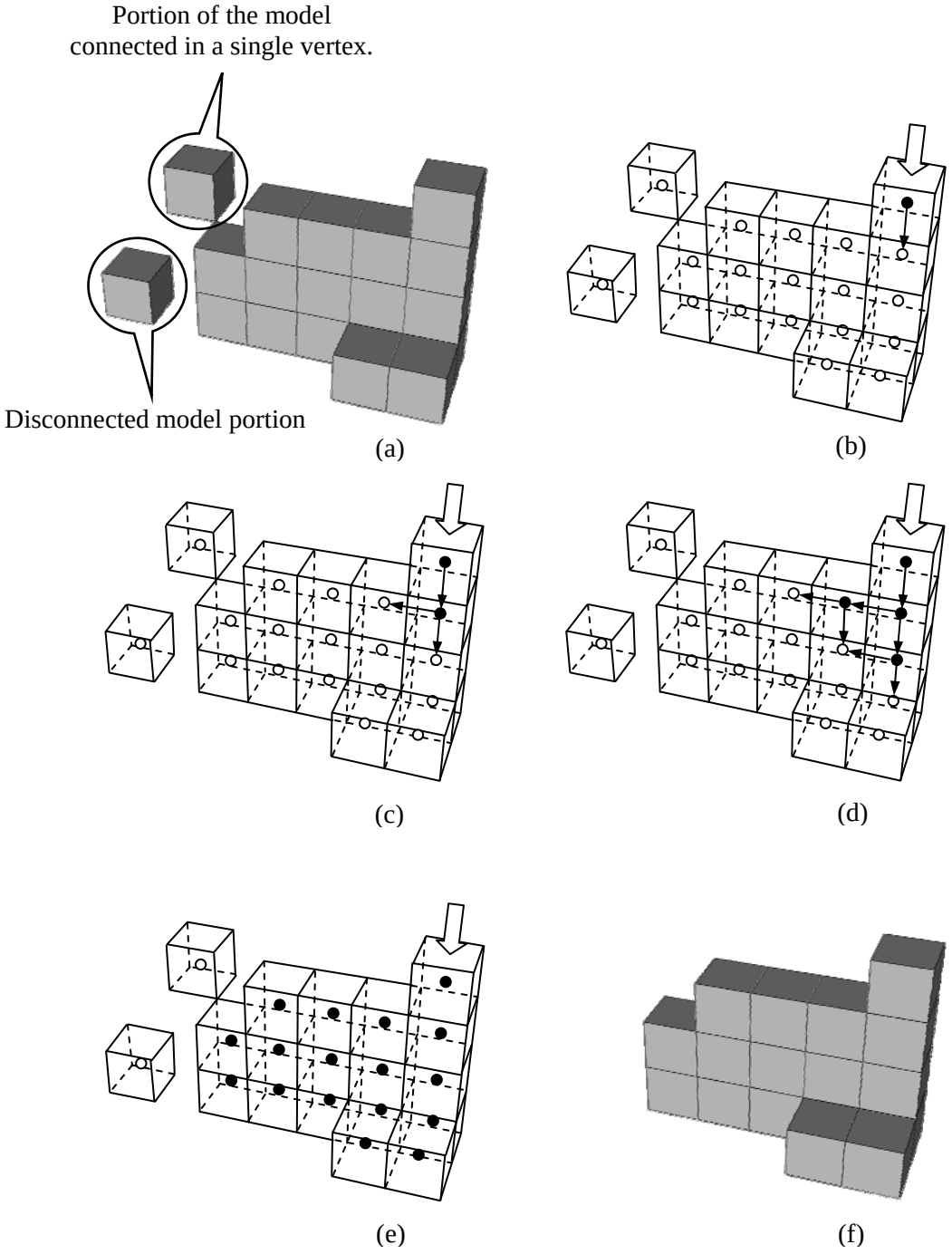

Figure 3: (a) Problems arising during the automatic model remeshing, (b to e) Geometry verification and fixing process via the identification of neighbour internal points, (f) Suitable model discretization after the deletion of the conflicting cubes.

Depending on the spatial distribution of the internal points, two problems may arise in the new boundary discretization (see Figure 3*a*): i) there are portions of the model defining "islands" disconnected from the main model boundary; and ii) there are portions of the model which are connected to the main model boundary via a single vertex or edge only. The disconnected cubes represent parts of model without loading carrying capacity which will lead to fatal errors in the BEM solution. Therefore, disconnected and not properly connected

portions of the model should be removed from the model. Cubes have to be connected via faces to the main model domain in order to be a valid one. This means, in order to represent a valid cube the distance of the associated internal point to its nearest neighbour has to be equal to the length of the cube edge.

The components not properly connected can have more than one element. The algorithm detecting of the disconnected components works by filling the main component with a valid flag, in a recursive neighbor-searching subroutine:

i. Select the internal point with the highest value for the topological derivative (note that this internal point always represents a loading carrying cube and thus will never be a disconnected one).
ii. Search for all the valid neighbors to the selected internal point (see Figure 3*b*). If the selected point has neighbors set the flag *hasNeighbor*=true.
iii. Select each of the internal points detected as valid neighbors and repeat the process in ii (See Figures 3*c*, 3*d* and 3*e*).
iv. Once the analysis finishes (that means no valid neighbors are detected) all the internal points with the value *hasNeighbor*=false are deleted. The process results in a valid BEM model (see Figure 3*f*).

The process results in a valid BEM model (see Figure 3*f*) by removing all the islands.

5 EXAMPLES

5.1 Two-dimensional Short Cantilever Beam

A two-dimensional problem was chosen for the first example in order to validate the implemented algorithm. It consists in a short cantilever beam of dimensions $30m \times 30m \times 1m$ constrained in the left side edge and with a vertical unit point load P=0.1 N applied at the top right vertex (see Figure 4). The problem was solved for two set of boundary conditions along the left edge: fully constrained (clamped, see Figure 4a) and with the displacements constrained in the x- and z-directions only (the first node has the displacements constrained in the y-direction in order to avoid rigid body displacements, see Figure 4b). In both cases the model was discretized using boundary elements of dimensions $1m \times 1m$, resulting in a 1,920 boundary elements mesh and 900 internal points. The material properties are E= 1Pa and ν=0.3. The problem was solved using a constant material removal rate η=0.55% of the initial model volume, what it is equivalent to removing 5 cubes per step.

Figure 5 illustrates the evolution of the model geometry together with the topological derivative and displacement results for the case of the clamped beam. The final geometry results after 159 steps. The optimized geometry contains 95 cubes which accounts for 10.5% of the material of the initial model.

The results of the optimization process for the case of the beam with left end partially restrained are depicted in Figure 6. It is interesting to compare these results to those of the first case. Since the left end of the beam is now free to displace in the y-direction, the optimized geometry develops a vertical arm parallel to the left edge of the beam. It is easy to see that this arm replaces the role of the clamped end in the first case, providing the structure rigidity in the vertical direction. The final optimized geometry is achieved after 144 steps and its volume is only 20% the initial one.

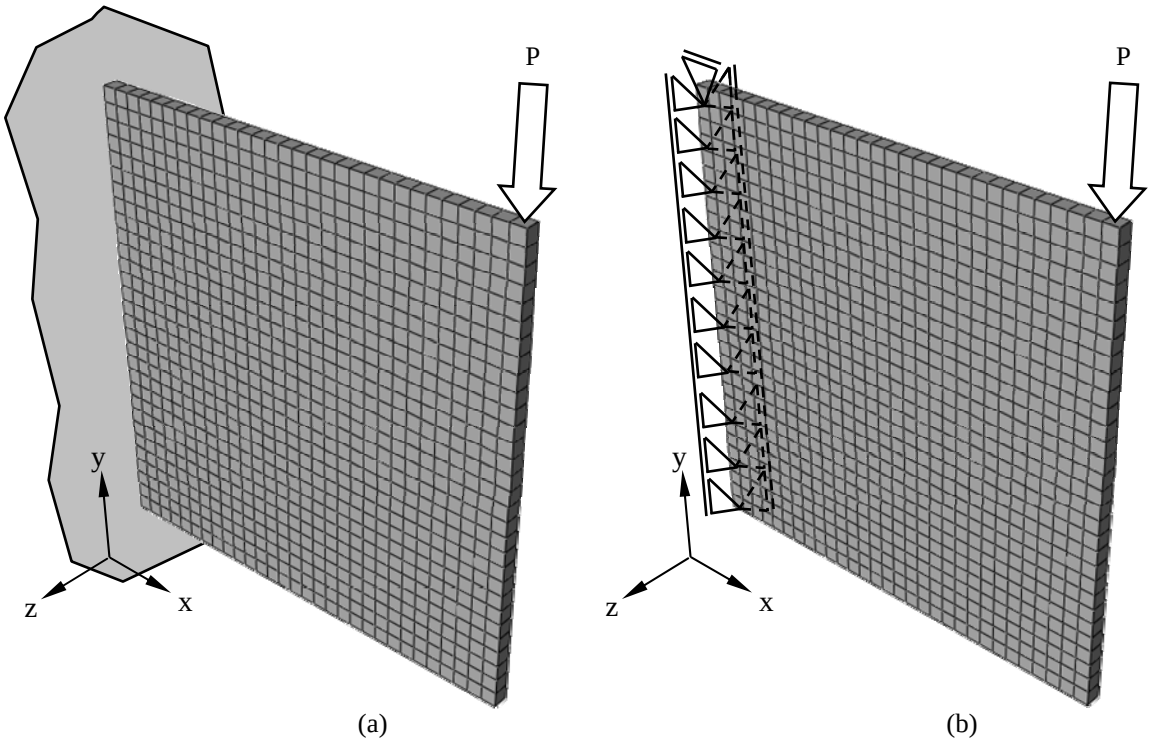

Figure 4: The short cantilever beam example: model geometry, boundary conditions and initial discretization for the (a) clamped and (b) partially constrained models.

5.2 Simply Supported Block Under Central Vertical Load

This second example consists in cube with the four vertices in the bottom face constrained in the vertical direction and free to slide in the horizontal plane. A load is applied in center of the top face (see Figure 7a). Problem dimensions are $40m \times 40m \times 10m$. Due to the symmetry of the structure, only one quarter of the problem was analyzed. The model was discretized using elements of dimensions $1m \times 1m$, resulting in a 600 boundary element mesh and 1,000 internal points. The load was chosen P=0.1 N and it was applied over one element. The displacement boundary condition at the bottom corner was also prescribed over a single element. The material properties were set the same to those of the first example.

The model was optimized using two different material removal rates: η=0.1% (one cube per step) and η=0.2% (two cubes per step). Figures 7b to 7d show the evolution of the model topology for the solution using η=0.1%. The final geometry is achieved after 960 steps. It consists in a four feet structure in a pyramidal shape joined by four horizontal supports. The volume of the optimized geometry is only 4% that of the initial one. Figures 7e and 7f illustrate the solutions reported by Ceá et al.(2000) and Novotny et al. (2007), who solved the problem using the fixed point and the topological derivative method respectively. In both cases the problem was solved using the finite element method coupled with adaptive meshing algorithms. It can be seen that although the difference in the problem dimensions (note that the reference solutions are for an initial cubic geometry), the optimized geometry computed in this work is in excellent agreement to those from the references.

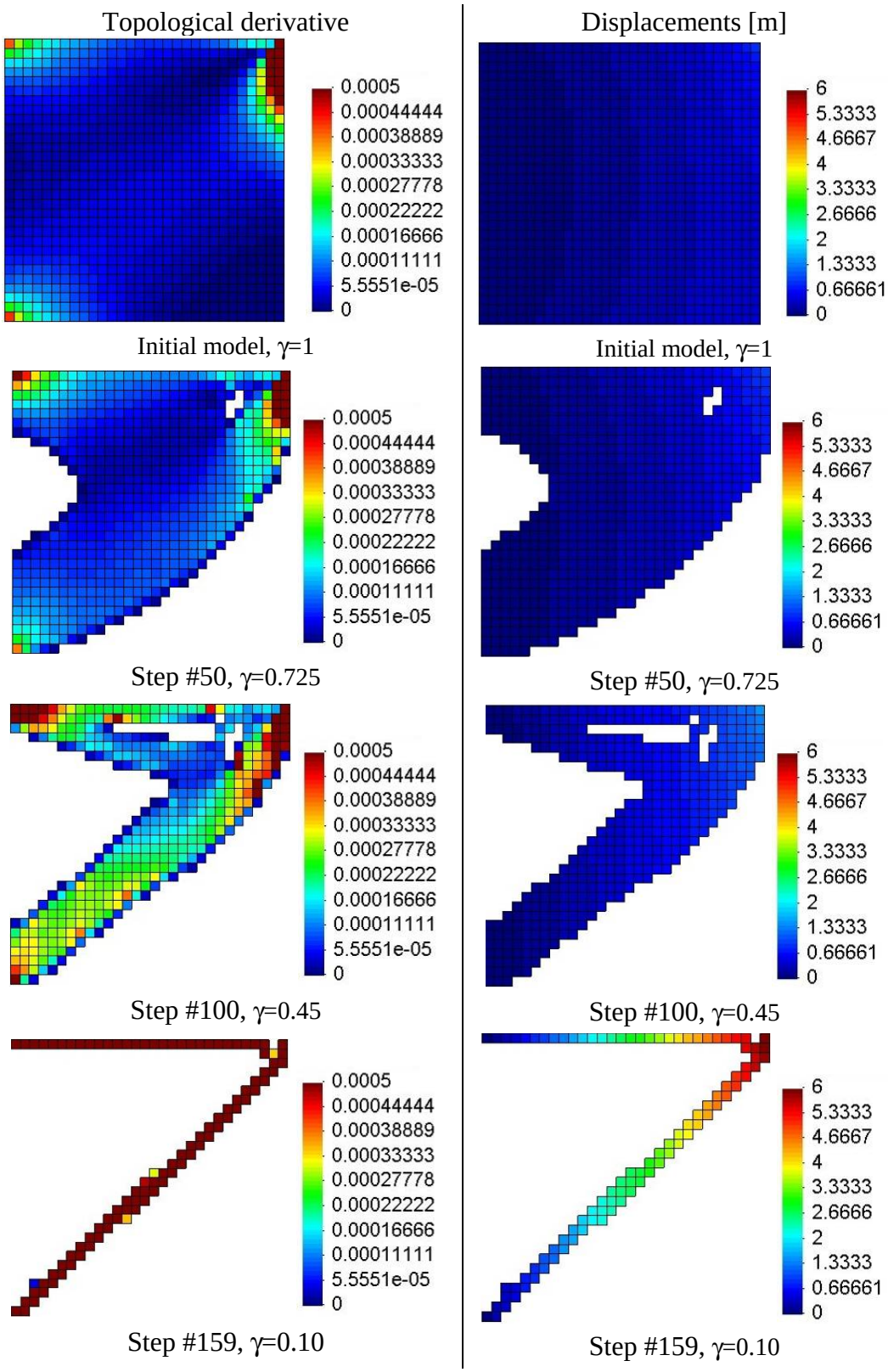

Figure 5: The short cantilever beam example: evolution of the model geometry and topological derivative and displacement results for the clamped case.

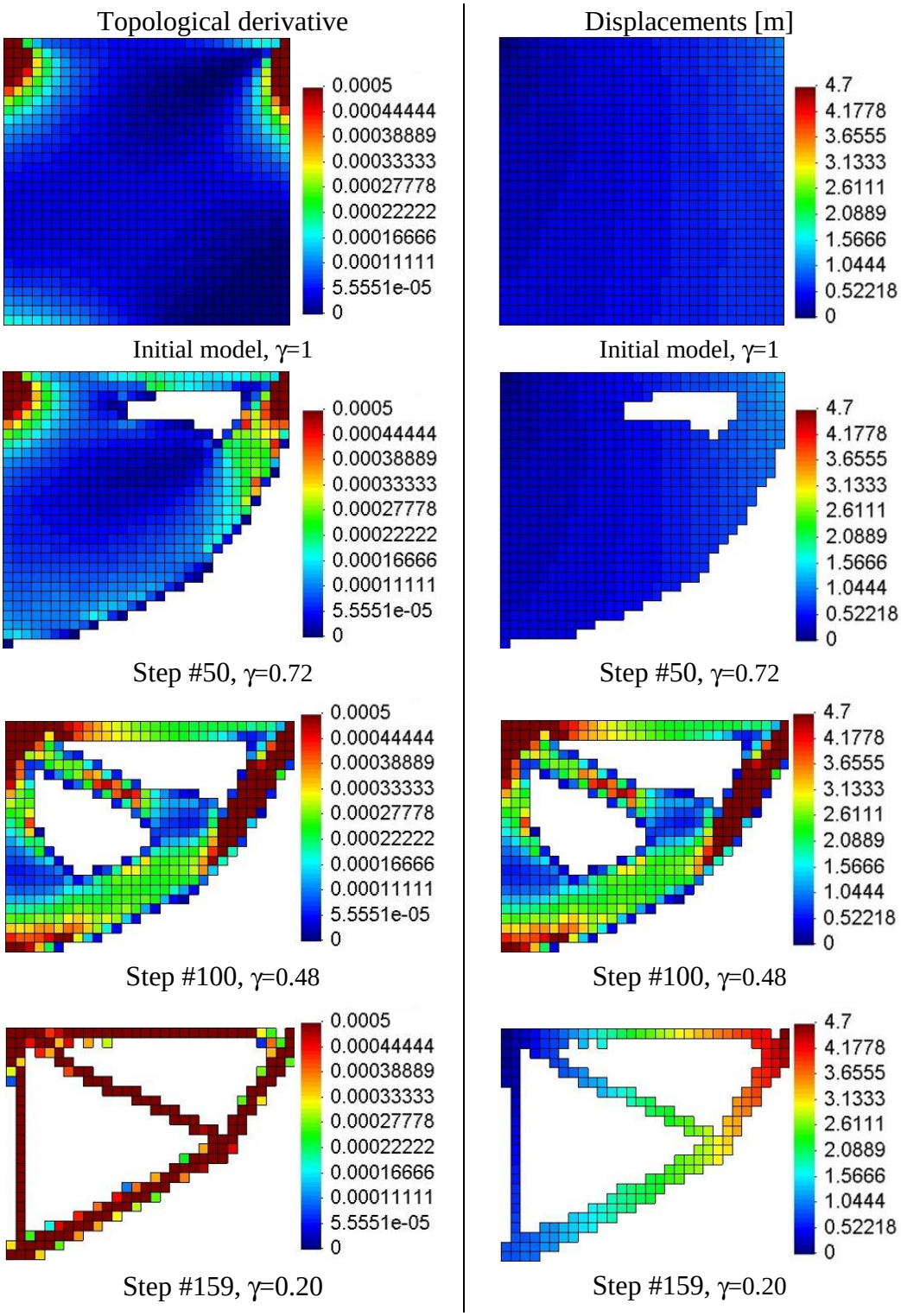

Figure 6: The short cantilever beam example: evolution of the model geometry and topological derivative and displacement results for the partially restrained case.

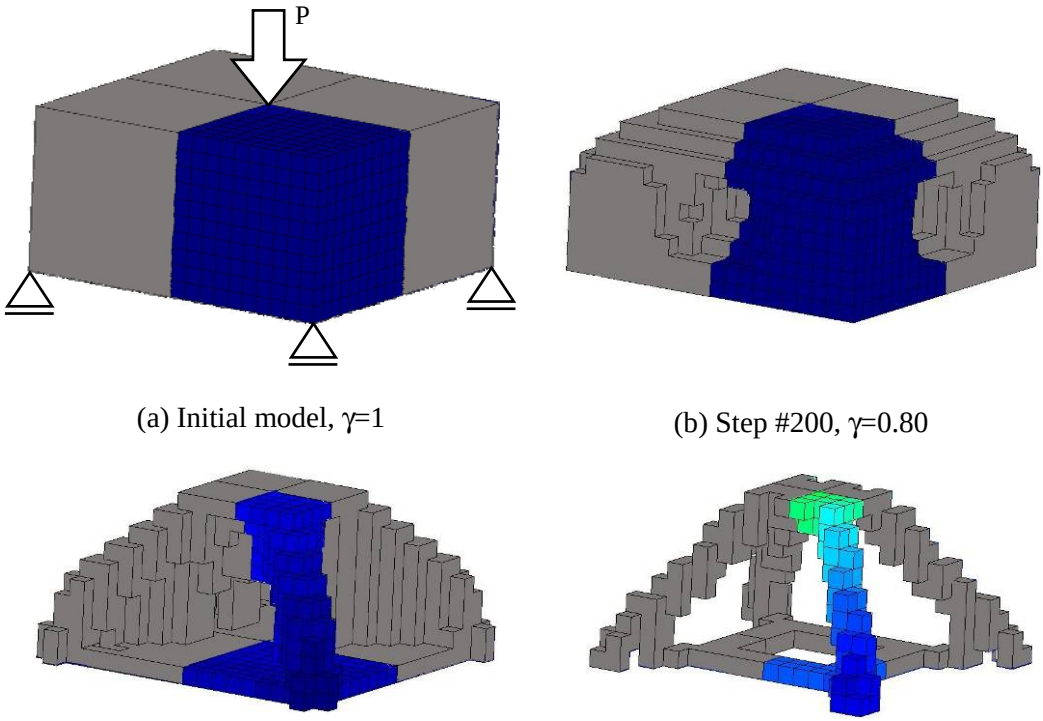

(a) Initial model, γ=1

(b) Step #200, γ=0.80

(c) Step #800, γ=0.20

(d) Step #960, γ=0.04

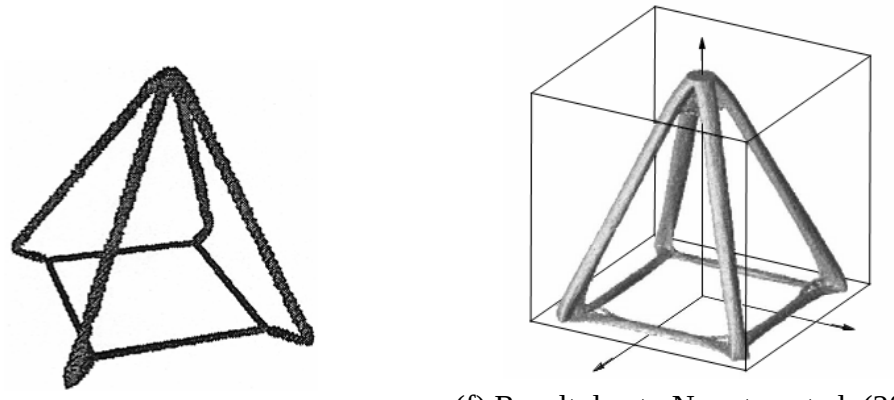

(e) Result due to Ceá et al. (2000) γ=0.01

(f) Result due to Novotny et al. (2007) γ=0.04

Figure 7: Simply supported block under central vertical load: (a to d) evolution of the model geometry and displacement results; (e and f): reference results.

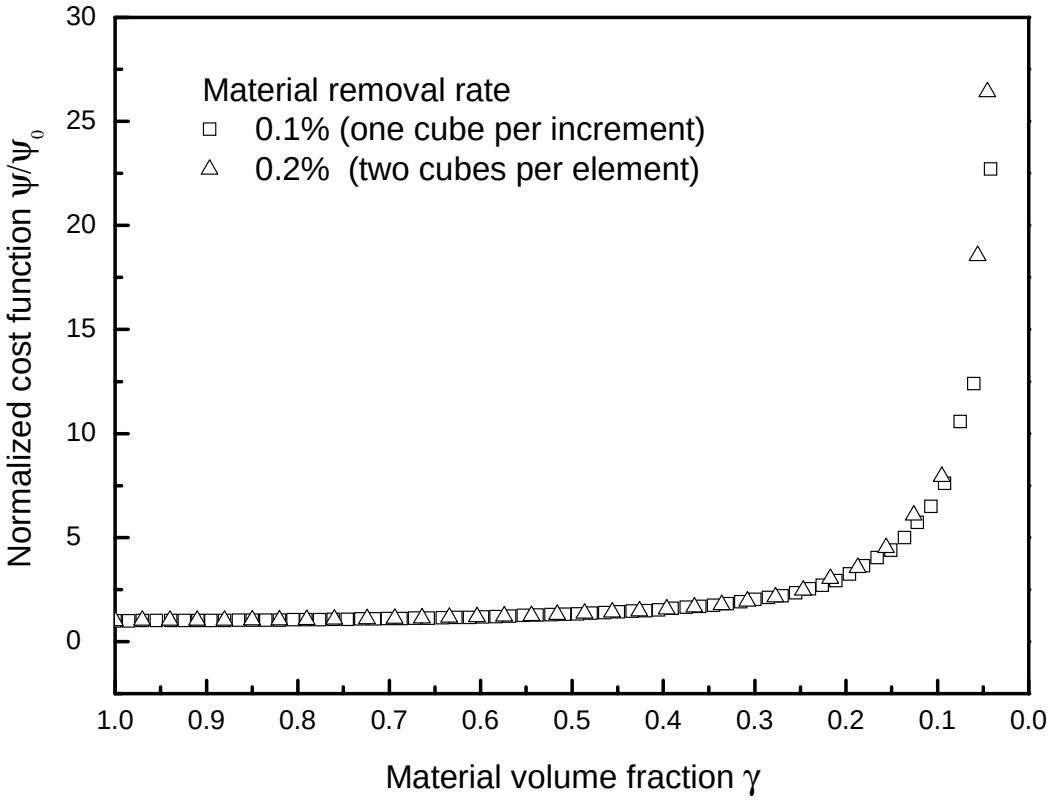

Figure 8: Simply supported block under central vertical load: evolution of the normalized cost functions in terms of the material volume fraction.

Similar results were obtained after 469 steps when the problem was solved using the η=0.2% material removal rate. The behavior of both solutions is compared in Figure 8, where the result of the normalized cost function, ψ/ψ_0, is plot as a function of the material volume fraction, γ. Note that since the total strain energy equals the work of the external forces, the plot in Figure 8 can also be interpreted as the relative increment of the problem compliance (the displacement of the load application point) with the decrement of the material volume fraction. It can be seen from Figure 8 that both solutions behave almost identically. This result suggest that in order to speed up the optimization process larger material removal rates could be used with no degradation of the problem solution.

Finally, an extra loading case with the four bottom corners clamped (displacements restrained in the three directions) was solved. In coincidence with the results reported by Ceá et al. (2000) the horizontal lattice between the four support disappear, and the optimal design is just made by four feet joined in the pyramidal structure.

6 CONCLUSIONS

An effective BEM implementation for the topological optimization of three-dimensional elastic structures was presented in this work using the total strain energy as cost function. The problem formulation is based on some recent results by Novotny et al. (2007), who introduced a new procedure for computing the topological derivative which allows overcoming some mathematical difficulties involved in its classical definition.

BEM models are discretized using constant quadrilateral elements and a regular array of

internal points. Each internal point is associated to a small material cube. The topological derivative is computed at internal points from the strain and/or stress results.

The optimization problem is solved incrementally. In every step the material removal is done by deleting from the model the internal points (and consequently the associated material cubes) with the lowest values of the topological derivative. The material removal is followed by a model remeshing and a checking procedure devised to avoid the occurrence of invalid BEM models. The process is repeated until the given stopping criterion (the goal minimum material volume fraction) is achieved.

The proposed method demonstrates the efficiency of boundary elements for topological optimization analysis, even when using low order elements. The developed implementation proves to be efficient and robust. Its performance is assessed by solving a number of examples.

ACKNOWLEDGEMENTS

This work has been partially supported by the CONICET and the Agencia de Promoción Científica of the República Argentina under grant PICT 12-14114 and the German Academic Exchange Service (DAAD).

REFERENCES

Aliabadi, M.H., and Wrobel, L.C. *The Boundary Element Method*. John Wiley & Sons, Chichister, UK, 2002.

Bendsøe, M.P. and Kikuchi, N. Generating optimal topologies in structural design using a homogenization method. *Comput. Methods Appl. Mech. Engrg*, 71:197-224, 1988.

Bendsøe, M.P. and Sigmund, O. *Topology Optimization*. Springer, Berlin, 2004.

Carretero Neches, L. and Cisilino, A.P. Topology optimization of 2D elastic structures using boundary elements. To appear in *Engineering Analysis with Boundary Elements* (The paper is available on line at the moment of the preparation of this manuscript).

Ceá, J., Gioan, A., and Michel, J. Adaptation de la méthode du gradient a a un probleme d'idenfification de domaine. In : *Lectures Notes in Computer Science*, Vol. 11, 371-402, Springer, Berlín, 1974.

Ceá, J., Garreau, S., Guillaume, P. and Masmoudi, M. The shape and topological optimization conection. *Comput. Methods Appl. Engrg.*, 188:713-726, 2000.

Cisilino, A.P. Topology Optimization of 2D potential problems using boundary elements. *Computer Modelling in Engineering & Sciences*, 15/2:99-106, 2006.

Eschenauer, H.A. and Olhoff, N. Topology optiomization of continuum structures: a review. *Appl. Mech. Rev.*, 54: 331-390, 2001.

Gurtin, M.E. *An Introduction to Continuum Mechanics*. Mathematics in Science and Engineering, Vol 158, Academic Press, 1981.

Mackerle, R. Topology and shape optimization of structures using FEM and BEM – a bibliography (1999-2001). *Finite Elements in Analysis and Design*, 39: 243-253, 2003.

Marczak, R.J. A Boundary element implementation for topology optimization of elastic structures. Proceddings of the *XXVII Iberian Latin-American Congress on Computational Methods in Engineering CILAMCE 2006*, Belem, Brazil, 2006.

Marczak, R.J. Topology optimization and boundary elements - a preliminary implementation for linear heat transfer. *Engineering Analysis with Boundary Elements*, 31/9: 793-802, 2007.

Novotny, A.A, Feijoo, R.A., Taroco, E. and Padra, C. C. Topological sensitivity analysis. *Comput. Methods Appl. Mech. Engrg.*, 192: 803-829, 2003.

Novotny, A.A, Feijoo, R.A., Taroco, E. and Padra, C. C. Topological sensitivity analysis for three-dimensional linear elasticity problem. *Computer Methods in Applied Mechanics and Engineering*, 196:41-44, 4354-4364, 2007.

Sadowsky M.A. and Sternberg E. Stress concentration around a triaxial ellipsoidal cavity. *Journal of Applied Mechanics*, 149-159, 1949.

Sigmund, O. and Peterson, J. Numerical inestabilities in topology optimization: A survey on procedures dealing with checkerboards, mesh dependencies and local minima. *Structural Optimization*, 16: 68-75, 1998.

Tanskanen, P. The evolutionary structural optimization method: theoretical aspects. *Computer Methods in Applied Mathematics and Engineering*, 190: 4081-4193, 2002.

Vemaganti, K. and Lawrence W.E. Parallel methods for optimality criteria-based topology optimization. *Comput. Methods Appl. Mech. Engrg*. 194: 3637–3667, 2005.

Wang, M.Y. and Wang, X. PDE-Driven level sets, shape sensitivity and curvature Flow for Structural Topology Optimization. *Computer Methods in Engineering Science*, 6/4: 373-395, 2004.

Wang, M.Y. and Wang, X. Structural shape and topology optimization using an implicit free boundary parametrization method. *Computer Methods in Engineering Science*, 13/2:119-147, 2006.